

Synthesis and characterization of polymeric microbeads loaded with lithium cobalt oxide nanoparticles for drug delivery and antibacterial applications

G. Ujwala¹, C. Madhavi², O. Sreekanth Reddy¹, M.C.S. Subha¹, K. Anitha¹

¹Department of Chemistry, Sri Krishnadevaraya University, Anantapur – 515 003, India

²Department of Polymer Science and Technology, Sri Krishnadevaraya University, Anantapur – 515 003, India

Abstract

The synthesis of biodegradable pH-responsive polymeric microbeads has high practical value for drug delivery applications. In the present study, we fabricate polymeric microbeads using sodium alginate and lithium cobalt oxide nanoparticles by an ionic-gelation technique for the controlled release of vancomycin. The developed microbeads were characterized by Fourier transform infrared spectroscopy, dynamic light scattering, X-ray diffraction analysis, and scanning electron microscopy. In vitro and swelling studies of the developed microbeads were carried out in both intestinal (pH 6.8) and gastric environments (pH 2.0) at 37 °C. The drug release studies and swelling study results suggested that developed microbeads were suitable for intestinal drug delivery. The drug release mechanism and kinetics were analyzed using Korsmeyer-Peppas and kinetics models (zero order, first order, and Higuchi). The generated microbeads showed antibacterial activity against *Streptococcus mutans*, *Lactobacillus acidophilus*, and *Bacillus subtilis*. Our generated microbeads warrant further development as drug carriers for the delivery of bioactive agents.

Keywords: Sodium alginate, Lithium cobalt oxide nanoparticles, Microbeads, Vancomycin, Antibacterial activity

1. Introduction

Nanotechnology is a branch of science that deals with materials with a diameter of one to a hundred nanometers. From basic material research to personal care, this technology has a wide range of uses today. As a result of their small size, nanoscience and nanotechnology have a profound impact on the medical area. When the particle size is reduced, its surface area increases, which in turn leads to improved bioavailability, decreased toxicity, increased solubility, and superior formulation properties of a drug. The drug's nanoscale size range may improve its performance in various dose forms. Rapid therapeutic efficacy, low dose, higher surface area, solubility, oral bioavailability, and lower patient variance are some of the perks that come along with using nanoparticles [1]. Due to their nanoscale diameters, passing through the smallest capillaries, high surface-volume ratio, high drug loading capacity, and multiple routes of administration, they are able to prevent quick clearance of medication[2].

Metal nanoparticles are very useful in drug delivery because of how their physical and chemical properties work together in a unique way [3]. Cobalt (Co) is an organometallic chemical or biopolymer, and it is most commonly found in the form of cobalt oxide[4]. In spite of its physiological role as a cofactor of vitamin B12, cobalt cannot be regarded only as an essential element. Surface modification confers antibacterial and anticancer properties to nanoparticles of cobalt oxide [5-7]. Li has been used as a substitute for salt to enhance the flavour of low Na⁺ diets and as a psychoactive drug for the treatment of manic-depressive illnesses. The results have ranged from the generation of severe and sometimes fatal Li intoxication to the successful management of severe mania [8].

Polymeric hydrogels may absorb vast amounts of water or biological fluids without disintegrating in the environment [9]. Due to their biodegradability and biocompatibility, polysaccharides have become viable choices for the synthesis of hydrogels in recent years. Hydrogels made of various polysaccharides have been extensively utilised in numerous domains, such as drug delivery systems, medicinal applications, enzyme immobilisation, and wastewater remediation[10]. Alginate is a linear, unbranched, and naturally occurring polysaccharide copolymer composed of 1,4-linked β-D-

mannuronic acid (M-block) and α -L-glucuronic acid (G-block) which are found in varying composition and sequence [11, 12]. One of the most interesting things about alginate is that it can bind to divalent ions to make hydrogel beads [13]. Vancomycin (VM) is a glycopeptide antibiotic discovered in the 1960s as a substitute for penicillin for the treatment of penicillinase-producing strains of *Staphylococcus aureus*. It is one of the most extensively used antibacterials in the world to treat severe gram-positive infections caused by *S. aureus* that is resistant to methicillin [14]. The main objective of the present study was to examine the capability of drug release from hydrogels under variations of pH of media with different ratios of CaCl_2 and MgCl_2 . In particular, this paper focuses in particular on drug release behaviours of polymer beads loaded with drugs and nanoparticles. The generated microbeads were characterised by SEM, XRD, DLS, and FTIR techniques. VM as a model drug was loaded into beads, and the release of drug from prepared microbeads was investigated by a dissolution experiment. The developed microbeads were tested for anti-bacterial activity against *Lactobacillus*, *Streptococcus*, and *Bacillus* species. The obtained results are presented in the paper.

2. Materials and methods

2.1 Materials

Sodium alginate, calcium chloride, magnesium chloride, sodium hydroxide, cobalt nitrate, and lithium nitrate were purchased from Sd.Fine chemicals, Mumbai, India. Vancomycin received as a gift sample from Aurbindo Pharma Ltd. Telangana, India. Double distilled water prepared in the laboratory was used throughout the experiment.

2.2 Synthesis of lithium cobalt oxide nanoparticles

Lithium cobalt oxide nanoparticles are synthesized by co-precipitation method, 3.68 g of cobalt nitrate and 0.69 g of lithium nitrate are dissolved in 100 mL distilled water under constant stirring for 2 hours. The resultant solution is treated with 20ml of 2M sodium hydroxide gives a precipitate, washed with distilled water times and then calcinated at 550 °C. The obtained NPs were stored in air-tight containers until further usage.

2.3 Synthesis of polymeric microbeads

300 mg of SA dissolved in 15 mL distilled water and stirred over night to get homogenous solution. To this solution, different ratios of VM and LiCoO_2 NPs were added (as given in Table 1) and subjected to sonication followed by stirring up to formation of homogenous solution. The resulting polymeric solution was dropped into different ratios of CaCl_2 and MgCl_2 solution (as given in Table 1). Instantaneously, the spherical beads were generated, and then they were held for 40 min for cross-linking purposes. The solution was decanted to collect the produced beads, which were then washed multiple times with distilled water to remove the drug from the surface. They were allowed to dry at 40°C in the oven for the whole night and then stored in a desiccator until further usage.

Table 1. Formulation, composition and encapsulation efficiency (%EE) of all samples.

Code	SA (mg)	VM (mg)	Distilled water (mL)	LiCoO_2 NPs (mg)	CaCl_2 : MgCl_2 (5%)	%EE
Ca	300	100	15	000	1:0	61.24
CaMg	300	100	15	000	1:1	63.25
CaMgNPs	300	100	15	100	1:1	64.12
2CaMg	300	100	15	000	2:1	62.23
Ca2Mg	300	100	15	000	1:2	66.16
Placebo	300	100	15	000	1:0	00.00

2.4. Characterization techniques

FTIR spectra of VM, placebo, LiCoO_2 NPs, Ca, CaMg, CaMgNPs, 2CaMg, and Ca2Mg microbeads were recorded in the range of 400-4000 cm^{-1} using model Bomem MB-3000. The X-ray diffraction of VM, placebo, LiCoO_2 NPs, Ca, CaMg, CaMgNPs, 2CaMg, and Ca2Mg microbeads were performed by a wide-angle X-ray diffractometer (Rigaku, Mini flex

600, JAPAN) with CuK α radiation ($\lambda= 1.54060$) at a scanning rate of 10°/min to determine the crystallinity. The scanning electron microscope (JOEL, IT500A, Japan) with an accelerated voltage of 20 kV was utilised in order to observe the morphological characteristics of the microbeads. Dynamic light scattering (Zetasizer ver. 7.10, Malvern Instruments Ltd., UK) instrument is used to find out the size of the NPs.

2.5. Antimicrobial activity

In vitro microbial activity of developed microbeads was determined using the disc diffusion method. Agar media was generated by dissolving 38 g of Muller Hinton Agar Medium (Hi-Media) in 1000 mL of distilled water. The dissolved media was autoclaved at 15 pounds of pressure and 121 °C Celsius for 15 minutes. The autoclaved media was cooled, thoroughly mixed, and placed onto petri dishes (25 mL per dish). The plates were swabbed with a culture of pathogenic bacteria (*Streptococcus mutans*, *Lactobacillus acidophilus*, and *Bacillus subtilis*). Using sterile forceps, five empty discs with a 6 mm diameter were created in the infected medium. Aqueous solutions of the test compounds were made at a concentration of 1 mg/mL and then 100 mL of the test sample was added to the wells. The plates were incubated at 37 °C for 24 h. After that, the zones of inhibition were measured in millimeters. 10 micrograms of vancomycin were employed as a standard control.

2.6. Encapsulation Efficiency

The percentage of encapsulation efficiency (percent EE) of VM-loaded microbeads was calculated using the prior literature's formula and method[15]. 10 mg of microbeads were precisely weighed and immersed for 24 h in 100 mL of phosphate buffer (pH 7.4, 5% absolute alcohol). After that, the solution is sonicated for ten minutes and then crushed to extract the drug from the microbeads. After that, the solution was filtered and the absorbance was measured using a UV-vis spectrophotometer at 281 nm. The following formula was used to calculate the percentage of encapsulation efficiency:

$$\% EE = \frac{W_t}{W_i} \times 100$$

Where W_t is total amount of VM in the microbeads and W_i is total amount of VM initially added during the preparation.

2.7. In-Vitro drug release studies and drug release kinetics

To evaluate the drug release studies of the produced microbeads, dissolution analysis was conducted with an eight-basket dissolution tester (Model: DS 2000, Make: LabIndia, Mumbai, India). 100 mg of microbeads are packed in dialysis bags and placed in 500 mL of pH 2.0 and 7.4 phosphate buffer solution (PBS) at 37 °C and 50 rpm. At regular intervals, 5 mL of dissolution media was taken out, analysed with a UV-Vis spectrophotometer at 281 nm, and then replaced with new media. Different models were used to fit the release curves of microbeads to determine their release kinetics (including the zero-order model, the first-order model, the Higuchi model, and the Korsmeyer–Peppas model). Correlation coefficients were used to determine the best model for drug release kinetics[16].

3. Results and Discussions

3.1. FTIR

The FTIR spectra of placebo, Ca, CaMg, 2CaMg, Ca2Mg, CaMgNPs and LiCoO₂ NPs are presented in Fig. 1. The VM shows a broad peak at 3415 cm⁻¹ (O-H and N-H stretching frequency), 1625 cm⁻¹ (C=O stretching frequency of the COOH group), 1506 cm⁻¹ (C=C stretching frequency), 1231cm⁻¹ (C-N stretching frequency), and 1122 cm⁻¹ (phenolic C-O stretching frequency). The FTIR spectra of placebo (plain SA microbeads) show a peak at 3411 cm⁻¹ (O-H stretching frequency), 1596 cm⁻¹ (C=O stretching frequency), and 1386 cm⁻¹ (C-O stretching frequency).[17] In comparing the drug-loaded microbeads and placebo, the stretching frequency of C=O at 1596 cm⁻¹ in placebo microbeads was shifted to 1606 cm⁻¹ in drug-loaded microbeads, indicating that the VM molecules interacted with the polymer matrix. In addition, 1122 cm⁻¹ is observed, which is due to the C-O stretching frequency of VM, which confirms that the drug has successfully loaded into the polymer matrix. The FTIR spectra of LiCoO₂ NPs showed characteristic peaks at 569, 675, 1387, and

1586 cm^{-1} , indicating the generation of LiCoO_2 NPs. A similar observation was reported by Khatun et al.[18] from their studies of the characterization of LiCoO_2 . When the CaMg NPs were compared to drug-loaded microbeads, new peaks at 589 and 676 cm^{-1} showed up in the CaMg NPs microbeads. This shows that the NPs are loaded into the polymer matrix successfully.

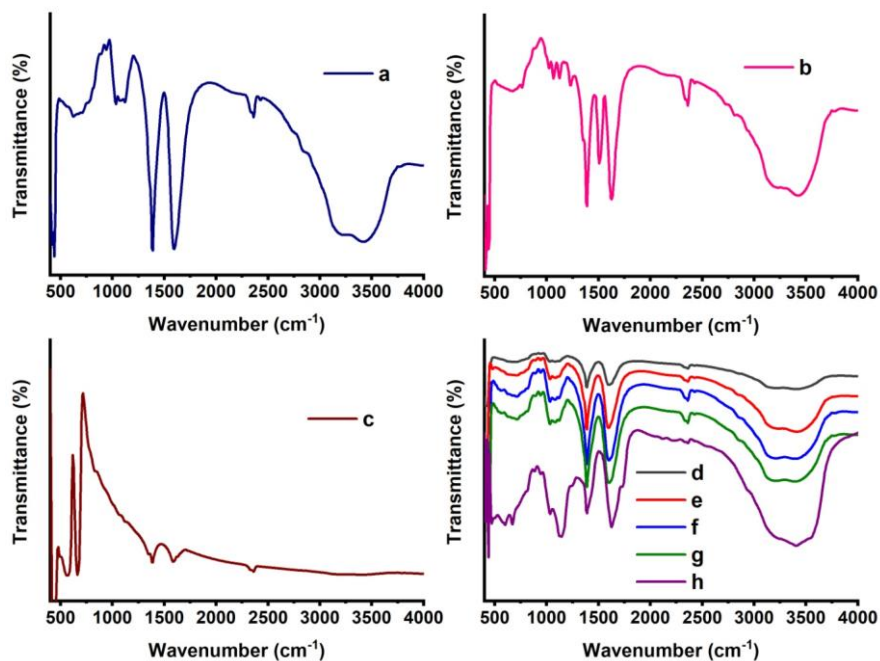


Fig. 1. FTIR spectra of (a), placebo (b), VM (c), LiCoO_2 NPs, (d)-(g) drug-loaded microbeads (Ca, CaMg , 2CaMg , and Ca_2Mg), and (h) NPs embedded drug-loaded microbeads (CaMg NPs).

3.2. XRD

The XRD diffractograms of placebo (a), Ca (b), CaMg (c), 2CaMg (d), Ca_2Mg (e), VM (f), LiCoO_2 NPs (g) and CaMg NPs are shown in Fig. 2. The XRD pattern of VM shows a halo at 2θ values of 10° to 35° , whereas these peaks are not found in drug-loaded microbeads, indicating that the drug molecules are molecularly dispersed in the polymer matrix. The XRD pattern of LiCoO_2 NPs shows major peaks at 19.0° , 31.4° , 37.0° , 38.5° , 44.8° , 59.4° , and 65.12° . These results are in good agreement with Aykut et al. [19] who found similar 2θ values for LiCoO_2 NPs in their study. Similarly, those peaks are observed in CaMg NPs microbeads, which confirms the presence of LiCoO_2 NPs in the polymer microbeads.

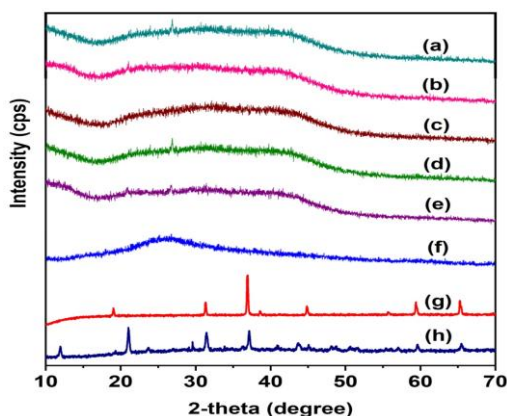


Fig. 2. XRD spectra of placebo (a), Ca (b), CaMg (c), 2CaMg (d), Ca_2Mg (e), VM (f), LiCoO_2 NPs (g) and CaMg NPs (h).

3.4. SEM and DLS

SEM examination was performed to determine the exterior structure of the generated microbeads, and the resulting pictures are shown in Figure 3. The results reveal that the microbeads are round and have a rough surface. It was intriguing that Ca2Mg had a more porous structure than other formulations. Due to the presence of a greater number of Mg^{2+} cations, the network has a porous, less rigid structure. The explanation for this is that Mg^{2+} ions are less tightly coupled with the polymeric matrix than Ca^{2+} ions, resulting in a more porous structure. Sanchez-Ballester et al. [20] also made a similar observation. In contrast, the Ca and 2CaMg formulations have a less porous character due to the development of a more rigid structure because Ca^{2+} ions are tightly coupled with the polymeric matrix. SEM scans revealed that the produced $LiCoO_2$ NPs (Figure 4a) have a size of 20-40 nanometers (nm). These results are further supported by the results of DLS analysis, in which the mean particle size of MNs is estimated to be 25-30 nm (Figure 4b). Based on SEM scans, the average size of microbeads was determined to be between 700 and 1000 μm .

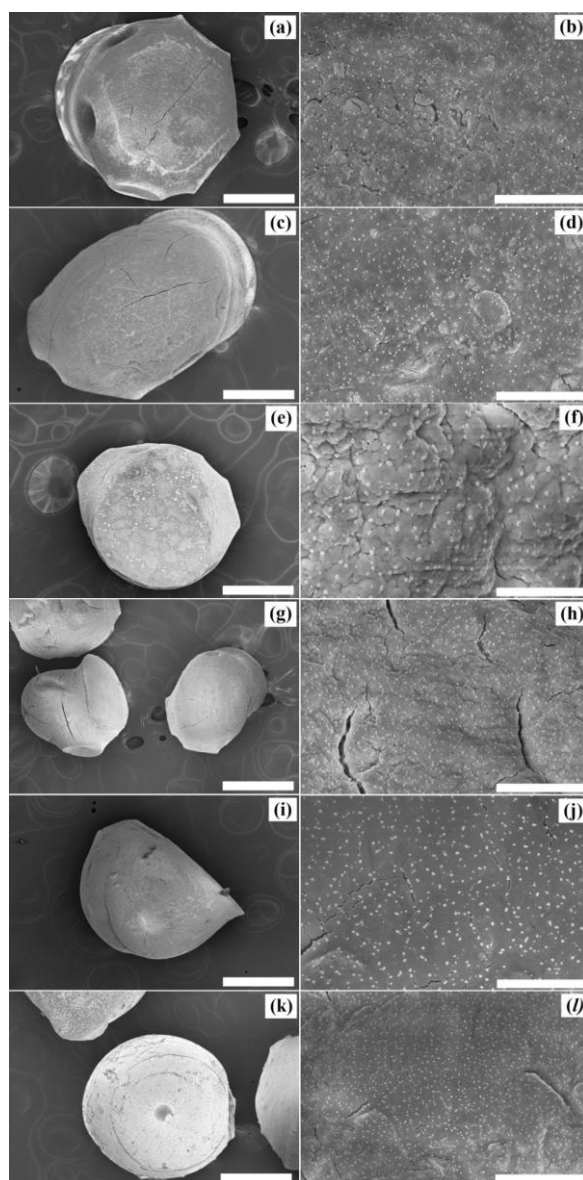


Figure 3. The topographical images of Ca (a & b), CaMg (c & d), CaMgNPs (e & f), Ca2Mg (g & h), 2CaMg (i & j), and placebo (k & l)

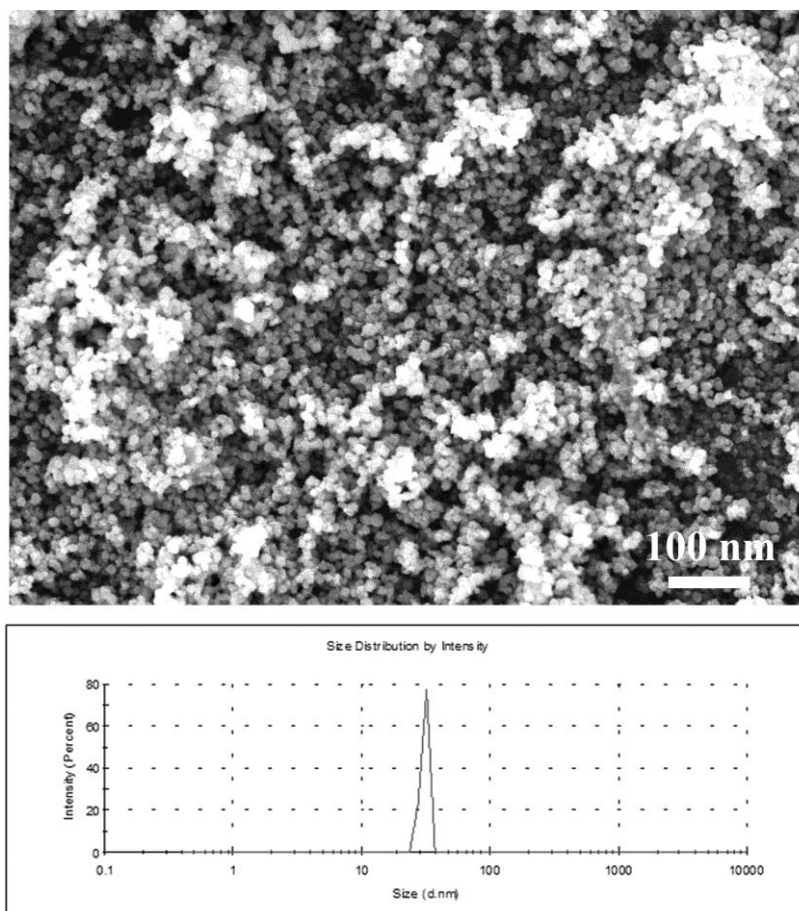


Figure 4. SEM images of LiCoO₂ NPs (a) with corresponding DLS image (b).

3.6. Encapsulation efficiency and *In vitro* release studies

The EE of VM varied across different formulations based on the number of cation ions present in the beads. The findings are summarised in Table 1. Compared to other formulations, the Ca2Mg formulation has a high EE. This is because its network has become less rigid, which makes it swell more and gives it a higher EE value.[21] *In vitro* release tests were done at 37 °C in PBS at pH 2.0 and 7.4, and the outcomes are depicted in Figure 5. It was discovered that the overall drug release rate is greater at pH 7.4 than it is at pH 1.2. This is because the carboxylate group has less interaction with the buffer at pH 7.4, which loosens the network and increases the permeability, allowing the drug to be released more easily.[22] At pH 2.0, the release rate was lower than at pH 7.4 as ionic-ionic repulsions were generated between H⁺ ions and the polymer matrix, preventing the entry of solvent into the polymer matrix. Consequently, the release rate was lowered.[23] This kind of pH response is helpful for drug delivery because it protects the drug molecules from the acidic environment of the stomach and makes it possible for them to be released from the carrier when they reach the intestines. Compared to other formulations, Ca2Mg has a higher release rate. This is because it has a more porous structure and the interactions between Mg²⁺ ions and alginates are weaker. This would make the Ca2Mg beads dissolve faster in the dissolution medium and make it easier for the drug molecules to leak out of the polymer matrix, whereas in the case of other formulations, they have a slower release rate due to their more rigid structure, which means VM molecules come out of the matrix at a slower rate.

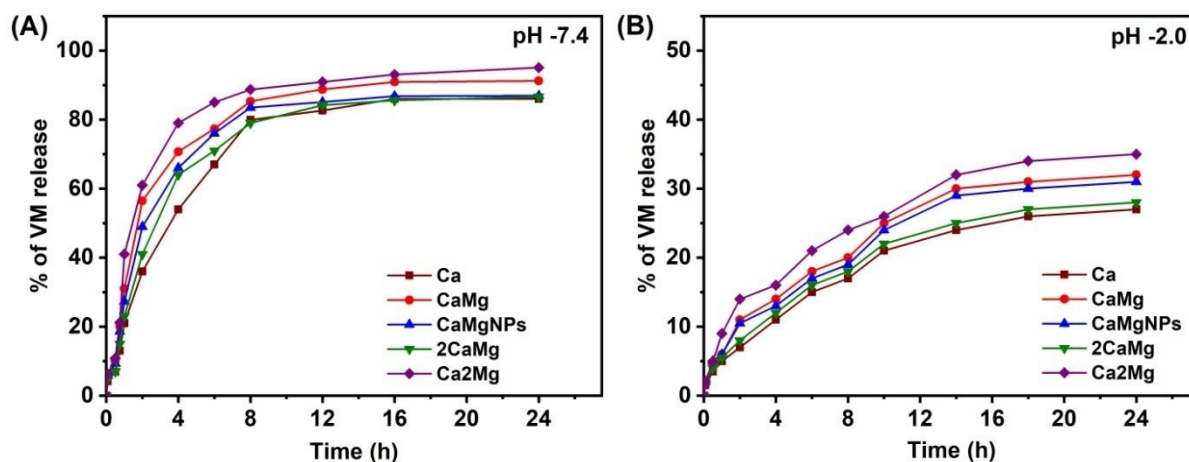


Figure 5. *In vitro* release profiles of developed microbeads in PBS at pH 7.4 (A) and pH 2.0 (B) at 37 °C.

3.7. Drug release kinetics

To determine the release kinetics of Ca, CaMg, CaMgNPs, 2CaMg, and Ca2Mg microbeads, release data were fitted into various kinetic models (zero order, first order, Higuchi model, and Korsmeyer-Peppas model), and their corresponding r^2 values are shown in Table 2. The release profiles of the microbeads that were made fit the Higuchi model. This means that the drug release process involves the PBS media penetrating into the alginate matrix and diffusing the drug molecules into the outside media. Furthermore, to determine the release mechanism of the synthesised microbeads, 60% of the release data was fitted to the Korsmeyer-Peppas equation, and the resulting n and r^2 values are presented in Table 2. The n values ranged from 0.493 to 0.790, showing that the produced microbeads followed a non-Fickian diffusion process.

Table 2. Release kinetics parameters of developed microbeads in PBS of pH 7.4 and 2.0 at 37 °C.

Code	pH	Zero		First		Higuchi		Korsmeyer-Peppas	
		K_0	r^2	K_1	r^2	K_H	r^2	n	r^2
Ca	7.4	5.032	0.592	0.133	0.979	20.555	0.924	0.790	13.369
	2.0	1.483	0.714	0.018	0.801	5.976	0.980	0.600	0.995
CaMg	7.4	5.522	0.396	0.190	0.985	22.934	0.897	0.669	20.301
	2.0	1.784	0.647	0.022	0.766	7.237	0.976	0.513	0.991
CaMgNPs	7.4	5.285	0.437	0.168	0.977	21.914	0.898	0.711	17.908
	2.0	1.720	0.61	0.021	0.773	6.964	0.977	0.498	0.991
2CaMg	7.4	5.153	0.545	0.147	0.980	21.172	0.917	0.775	14.911
	2.0	1.548	0.669	0.019	0.769	6.270	0.981	0.563	0.996
Ca2Mg	7.4	5.718	0.347	0.213	0.992	23.818	0.896	0.626	22.933
	2.0	1.960	0.551	0.025	0.703	8.014	0.973	0.493	0.983

3.8. Antibacterial activity

Finally, to demonstrate the antibacterial activity of VM-loaded microbeads, they were examined by using *Streptococcus mutans*, *Lactobacillus acidophilus*, and *Bacillus subtilis* as models (Figure 6). The developed microbeads exhibit antimicrobial activity against *Streptococcus mutans*, *Lactobacillus acidophilus*, and *Bacillus subtilis*. From Table 3, it was observed that CaMgNPs has shown a good inhibition zone than the other microbeads, which is due to the presence of LiCoO₂ NPs along with VM in the polymer matrix. In addition, pure NPs also shows the inhibition activity against all bacterial models.

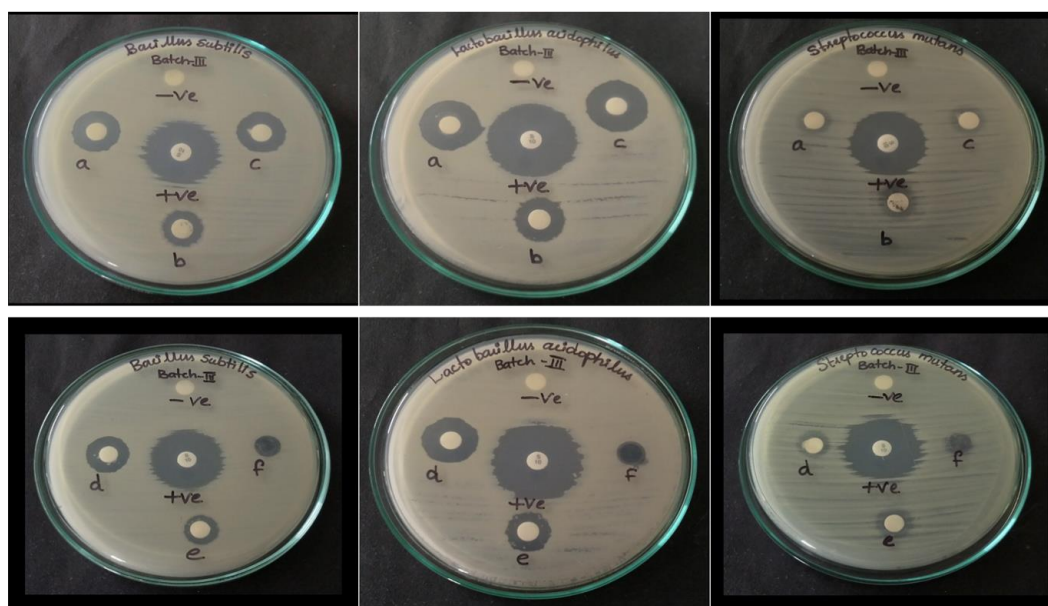


Fig. 4. (A) Images showing the zone of inhibition induced by developed microbeads [(a) Ca2Mg, (b) CaMg, (c) CaMgNPs, (d) 2CaMg, (e) Ca and (f) LiCoO₂ NPs] for *Streptococcus mutans*, *Lactobacillus acidophilus*, and *Bacillus subtilis*.

Table 3. Diameter of zones of inhibition (mm) of given compounds against microorganisms after the incubation period of 24h.

Microbial species	Positive Control	Inhibition Zone (mm)					
		Ca2Mg	CaMg	CaMgNPs	2CaMg	Ca	LiCoO ₂ NPs
<i>S.Mutans</i>	25	10	12	13	11	12	9
<i>L.Acidophilus</i>	23	19	15	19	16	14	8
<i>B.Subtilis</i>	24	14	12	15	14	12	10

4. Conclusion

In this study, we report the generation of microbeads using SA and LiCoO₂ NPs as carriers for VM release. The microbeads were prepared using a simple ionic gelation method for the controlled release of VM. FTIR studies confirmed the interactions between VM and the polymer network. X-RD results confirmed the molecular dispersion of VM in the matrix. SEM study indicated the spherical and rough surface of the matrix. DLS reveals the sizes of the developed NPs are in the range of 25-30 nanometres. The developed microbeads show antibacterial activity against *Streptococcus mutans*, *Lactobacillus acidophilus*, and *Bacillus subtilis*. The presence of LiCoO₂ NPs showed good antibacterial activity than the

other microbeads. *In vitro* release studies suggested that the microbeads developed were suitable for intestinal drug delivery and followed non-fickian type diffusion mechanism.

.Conflict of Interest

The authors declare no conflict of interest.

References

- [1] A. Suttee, G. Singh, N. Yadav, R.P. Barnwal, N. Singla, K.S. Prabhu, V. Mishra, A review on status of nanotechnology in pharmaceutical sciences, *International Journal of Drug Delivery Technology*, 9 (2019) 98-103.
- [2] M. Ghaffari, J.E.N. Dolatabadi, *Nanotechnology for pharmaceuticals, Industrial Applications of Nanomaterials*, Elsevier2019, pp. 475-502.
- [3] S.R. Obireddy, W.-F. Lai, ROS-Generating Amine-Functionalized Magnetic Nanoparticles Coupled with Carboxymethyl Chitosan for pH-Responsive Release of Doxorubicin, *International journal of nanomedicine*, 17 (2022) 589-601.
- [4] K. Wang, J.-J. Xu, H.-Y. Chen, A novel glucose biosensor based on the nanoscaled cobalt phthalocyanine–glucose oxidase biocomposite, *Biosensors and Bioelectronics*, 20 (2005) 1388-1396.
- [5] E. Papis, F. Rossi, M. Raspanti, I. Dalle-Donne, G. Colombo, A. Milzani, G. Bernardini, R. Gornati, Engineered cobalt oxide nanoparticles readily enter cells, *Toxicology Letters*, 189 (2009) 253-259.
- [6] V. Gupta, V. Kant, A. Sharma, M. Sharma, Comparative assessment of antibacterial efficacy for cobalt nanoparticles, bulk cobalt and standard antibiotics: A concentration dependant study, *Наносистемы: физика, химия, математика*, 11 (2020) 78-85.
- [7] S. Chattopadhyay, S.P. Chakraborty, D. Laha, R. Baral, P. Pramanik, S. Roy, Surface-modified cobalt oxide nanoparticles: new opportunities for anti-cancer drug development, *Cancer Nanotechnology*, 3 (2012) 13-23.
- [8] I. Singer, D. Rotenberg, Mechanisms of lithium action, *New England Journal of Medicine*, 289 (1973) 254-260.
- [9] Z. Mohamadnia, M. Zohuriaan-Mehr, K. Kabiri, A. Jamshidi, H. Mobedi, Ionically cross-linked carrageenan-alginate hydrogel beads, *Journal of Biomaterials Science, Polymer Edition*, 19 (2008) 47-59.
- [10] G.R. Mahdavinia, Z. Rahmani, S. Karami, A. Pourjavadi, Magnetic/pH-sensitive κ -carrageenan/sodium alginate hydrogel nanocomposite beads: preparation, swelling behavior, and drug delivery, *Journal of Biomaterials Science, Polymer Edition*, 25 (2014) 1891-1906.
- [11] S.R. Obireddy, W.-F. Lai, Multi-Component Hydrogel Beads Incorporated with Reduced Graphene Oxide for pH-Responsive and Controlled Co-Delivery of Multiple Agents, *Pharmaceutics*, 13 (2021) 313.
- [12] S.R. Obireddy, M. Chintha, C.R. Kashayi, K.R.K.S. Venkata, S.M.C. Subbarao, Gelatin-Coated Dual Cross-Linked Sodium Alginate/Magnetite Nanoparticle Microbeads for Controlled Release of Doxorubicin, *ChemistrySelect*, 5 (2020) 10276-10284.
- [13] J. Supramaniam, R. Adnan, N.H. Mohd Kaus, R. Bushra, Magnetic nanocellulose alginate hydrogel beads as potential drug delivery system, *International Journal of Biological Macromolecules*, 118 (2018) 640-648.
- [14] A. Marsot, A. Boulamery, B. Bruguerolle, N. Simon, Vancomycin, *Clinical pharmacokinetics*, 51 (2012) 1-13.
- [15] S.R. Obireddy, W.-F. Lai, Preparation and characterization of 2-hydroxyethyl starch microparticles for co-delivery of multiple bioactive agents, *Drug Delivery*, 28 (2021) 1562-1568.
- [16] M. Chintha, S.R. Obireddy, P. Areti, S. Marata Chinna Subbarao, C.R. Kashayi, J.K. Rapoli, Sodium alginate/locust bean gum-g-methacrylic acid IPN hydrogels for “simvastatin” drug delivery, *Journal of Dispersion Science and Technology*, 41 (2020) 2192-2202.
- [17] O.S. Reddy, M.C.S. Subha, T. Jithendra, C. Madhavi, K.C. Rao, Fabrication and characterization of smart karaya gum/sodium alginate semi-IPN microbeads for controlled release of D-penicillamine drug, *Polymers and Polymer Composites*, 29 (2020) 163-175.
- [18] F. Khatun, M.A. Gafur, M.S. Ali, M.S. Islam, M.A.R. Sarker, Impact of Lithium Composition on Structural, Electronic and Optical Properties of Lithium Cobaltite Prepared by Solid-state Reaction, *Journal of Scientific Research*, 6 (2014) 217-231.

- [19] Y. Aykut, B. Pourdeyhimi, S.A. Khan, Synthesis and characterization of silver/lithium cobalt oxide (Ag/LiCoO₂) nanofibers via sol–gel electrospinning, *Journal of Physics and Chemistry of Solids*, 74 (2013) 1538-1545.
- [20] N.M. Sanchez-Ballester, I. Soulaïrol, B. Bataille, T. Sharkawi, Flexible heteroionic calcium-magnesium alginate beads for controlled drug release, *Carbohydrate Polymers*, 207 (2019) 224-229.
- [21] O. Srekanth Reddy, M.C.S. Subha, T. Jithendra, C. Madhavi, K. Chowdoji Rao, Curcumin encapsulated dual cross linked sodium alginate/montmorillonite polymeric composite beads for controlled drug delivery, *Journal of Pharmaceutical Analysis*, 11 (2021) 191-199.
- [22] S. Eswaramma, K.S.V.K. Rao, Synthesis of dual responsive carbohydrate polymer based IPN microbeads for controlled release of anti-HIV drug, *Carbohydrate Polymers*, 156 (2017) 125-134.
- [23] S. Takka, A. Gürel, Evaluation of Chitosan/Alginate Beads Using Experimental Design: Formulation and In Vitro Characterization, *AAPS PharmSciTech*, 11 (2010) 460-466.